Journal Name

ARTICLE TYPE

Cite this: DOI: 10.1039/xxxxxxxxxx

Electronic Supplementary Information: A Reaction Model on Self-assembly Process of Octahedron-Shaped Coordination Capsule

Yoshihiro Matsumura,[a] Shuichi Hiraoka,[b] and Hirofumi Sato*[a,c]

Received Date
Accepted Date

DOI: 10.1039/xxxxxxxxxx

www.rsc.org/journalname

This document provides additonal information on the computations.

Contents

1 Enumeration of species

1.1 Algorithm

The algorithm enumerating all the chemical species appearing in the self-assembly process is explained in this section. We assume that all the species including reactant, product and intermediates satisfy the following rules.

- Each species consists of some or all of Pd, L and Py.
- Pd and L are respectively allowed to occupy one of six apexes and eight faces (Pd1-Pd6 and L1-L8 in the Figure (S1)) in the octahedron geometry of $[Pd_6L_8]^{12+}$.
- Pd is always coordinated by four components (Py or L).
- The maximum bonding numbers of L and Py are three and one, respectively. The minimum is zero.
- All of Pd, L and Py adjoin to another component. All of them compose one molecule.

In practice, the following algorithm was used to generate candidates. Note that the neighbouring Pd···L pair is strictly distinguished from Pd-L bond in the present treatment. For example, in the pre-final product $[Pd_6L_8Py]^{12+}$, one Pd is bound with Py instead of L though these Pd and L are neighbouring each other.

P1: Initially, Pd and L are respectively placed at Pd1 and L1 sites.

P2: Starting from the prepared (parent) structure, new structures are derivatively generated by the following procedures of (a), (b) and (c), respectively. If more than one parent structures are available, all of them are examined one by one.

(a) A new Pd is placed at one of vacant Pd sites. If this Pd is neighbouring a pre-existing L, new Pd-L bond between them is formed and this structure is registered as a new one. If this Pd is neighbouring more than one

[a] *Department of Molecular Engineering, Kyoto University, Kyoto 615-8510, Japan, E-mail: hirofumi@moleng.kyoto-u.ac.jp*
[b] *Department of Molecular Engineering, Kyoto University, Kyoto 615-8510, Japan*
[c] *Elements Strategy Initiative for Catalysts and Batteries, Kyoto University, Kyoto, Japan*

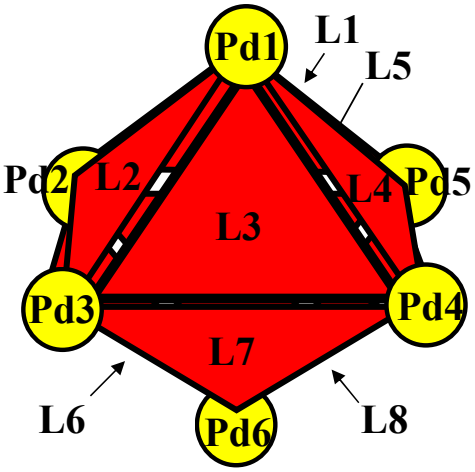

Fig. S1 Pd and L sites in octahedron-shaped product $[Pd_6L_8]^{12+}$.

L, each structure with different new Pd-L bond is individually registered. The procedure is repeated over all the vacant Pd sites.

(b) A new L is placed at one of vacant L sites. If this L is neighbouring a pre-existing Pd, new Pd-L bond between them is formed and this structure is registered as a new one. If this L is neighbouring more than one Pd, each structure with different new Pd-L bond is individually registered. The procedure is repeated over all the vacant L sites.

(c) All of pre-existing Pd$\cdots$L pairs (24 as the maximum) are examined. If Pd and L are neighbouring each other without a bond, this pair is replaced with a new bond. If there are more than one Pd$\cdots$L pairs, each structure with different new Pd-L bond is individually registered. The procedure is repeated over all the pairs.

A proper numbers of Py's are then added so as to satisfy the Pd coordination rule. In each step through (a)–(c), Pd$\cdots$L pair is examined one by one, and one Pd-L bond formation generates a new structure. Eventually, many new structures are registered, but duplicated ones are removed through the checking of O_h symmetry operations. Finally, the obtained structures are stored.

P3: If all the structures reach Pd_6L_8, the procedure is terminated. Otherwise, going back to P2, and all the stored structures are used as the parent ones.

Together with $PdPy_4$, L, and Py, total 170047 structures were obtained. All the structures were then grouped into their compositions; $Pd_aL_bPy_c$ or "*abc*". The total number was 156. The species are essentially identified only with their composition, but geometrical feature is partly taken into consideration. For example, L_2 is not generated by the present procedure.

1.2 Other types of intermediates

One might consider a possibility to generate larger-size intermediates, $[Pd_aL_bPy_c]^{2a+}$ $(a > 6)$, in reality. However, these intermediates are expected to be less important from a viewpoint of kinetics. In fact, the populations of large linear oligomers such as $[Pd_5L_5Py_{11}]^{10+}$ and $[Pd_6L_6Py_{13}]^{12+}$ are as much as 10^{-3} % and 10^{-4} % metal distributions at peak around a few min (short time), and rapid convergence to dominant intermediates was observed in calculations. Hence, larger ones $(a > 6)$ can be reasonably excluded. It is also important to note that the experimentally observed n,k values are converged to those of $[Pd_6L_8Py]^{12+}$ and almost unchanged (especially n) at long time, implaying that the larger intermediates do not produced.

2 Master equation approach

In the present study, time evolution of reaction is simulated based on master equation. A robust and accurate stochastic method to solve the master equation [1,2,4,5] is useful to explore the entire process of molecular self-assembly. It should be mentioned that D'Orsogna et al. [1,2] reported a remarkable difference between results from the master equation based approach and those from conventional rate equation based approach, called Becker-Döring equation [3], using physical toy model of self-assembly.

The reactant species in all the reactions are chosen from the intermediates shown in Figure 1 of the main text. The products must be presented in the figure, too. In the present study, a set of numbers of all the chemical species A (N_A) is introduced to represent a state of the system,

$$\{N\} \equiv \{N_{PdPy_4}, N_L, \cdots, N_{Pd_aL_bPy_c}, \cdots, N_{Pd_6L_8}\}. \quad \text{(S1)}$$

In other words, a vector consisting of 156 elements is considered.

The probability distribution function of the state $\{N\}$ at time t is defined as $P(\{N\},t)$ [1,2], and the amount of chemical species at time t is calculated as the mean numbers using $P(\{N\},t)$,

$$\langle N_A(t)\rangle = \sum_{\{N\}} N_A P(\{N\},t). \quad \text{(S2)}$$

The time evolution is described by master equation on $P(\{N\},t)$.

$$\frac{d}{dt}P(\{N\},t) = \sum_{\{N'\}\neq\{N\}} T(\{N'\}\to\{N\})P(\{N'\},t) - \sum_{\{N''\}\neq\{N\}} T(\{N\}\to\{N''\})P(\{N\},t). \quad \text{(S3)}$$

In the right hand side of Eq. (S3), the first and second terms respectively denote increase and decrease of the present probability of the state $(\{N\})$. The summation $(\sum_{\{N'\}\neq\{N\}})$ is over all the possible states except for $\{N\}$, and $T(\{N\}\to\{N'\})$ is transition probability from $\{N\}$ to $\{N'\}$.

Transition probability T is directly related to the rate of the elementary reactions, (i)−(iv), as explained in section 4. T was computed if $\{N\}\to\{N'\}$ corresponds to one of them, or set to "0" otherwise. Eq. (S3) was simulated using a kinetic Monte Carlo (kMC) or residence time algorithm [4]. We would like to emphasize that the present master-equation-based approach provides microscopic description of the reaction, which is different from conventional rate equation as described in the following section.

3 Relation between master equation and rate equation

The master equation is not the same as rate equation. In this section, the relationship between them is discussed for bimolecular reaction and unimolecular reaction[1,2].

3.1 Bimolecular reaction

The simplest bimolecular reaction is considered:

$$\text{molecule I} + \text{molecule II} \rightarrow \text{molecule III}.$$

In the master equation, the state of the system is described by a set of numbers ($\{N_\mathrm{I}, N_\mathrm{II}, N_\mathrm{III}\}$), where $N_\mathrm{I}, N_\mathrm{II}$ and N_III are respectively the numbers of molecules I, II and III. The equation describes the time evolution of the probability distribution function, $P(\{N_\mathrm{I}, N_\mathrm{II}, N_\mathrm{III}\}, t)$.

$$\frac{dP(\{N_\mathrm{I}, N_\mathrm{II}, N_\mathrm{III}\}, t)}{dt} = p(N_\mathrm{I}+1)(N_\mathrm{II}+1)P(\{N_\mathrm{I}+1, N_\mathrm{II}+1, N_\mathrm{III}-1\}, t) - pN_\mathrm{I}N_\mathrm{II}P(\{N_\mathrm{I}, N_\mathrm{II}, N_\mathrm{III}\}, t). \quad \text{(S4)}$$

The first term of the right hand side contributes the increase of probability of $P(\{N_\mathrm{I}, N_\mathrm{II}, N_\mathrm{III}\}, t)$, corresponding to the variation, $\{N_\mathrm{I}+1, N_\mathrm{II}+1, N_\mathrm{III}-1\} \rightarrow \{N_\mathrm{I}, N_\mathrm{II}, N_\mathrm{III}\}$. The rate is given by the product of the constant p representing the rate of this reaction, the numbers of each species, and the probability of the state, $P(\{N_\mathrm{I}+1, N_\mathrm{II}+1, N_\mathrm{III}-1\}, t)$. The second term is the variation $\{N_\mathrm{I}, N_\mathrm{II}, N_\mathrm{III}\} \rightarrow \{N_\mathrm{I}-1, N_\mathrm{II}-1, N_\mathrm{III}+1\}$, contributing to the decrease of probability, $P(\{N_\mathrm{I}, N_\mathrm{II}, N_\mathrm{III}\}, t)$. Note that both of them produce molecule III. Because the backward reaction is separately treated, and not involved in Eq. (S4). The mean number at time t is introduced as follows,

$$\langle N_\mathrm{X} \rangle = \sum_{N_\mathrm{I}, N_\mathrm{II}, N_\mathrm{III}} N_\mathrm{X} P(\{N_\mathrm{I}, N_\mathrm{II}, N_\mathrm{III}\}, t), \quad (\mathrm{X} = \mathrm{I}, \mathrm{II}, \mathrm{III}) \quad \text{(S5)}$$

A relationship to the conventional rate equation can be understood by computing the time evolution of molecule III. Taking the sum in both sides of Eq. (S4),

$$\begin{aligned}\frac{d\langle N_\mathrm{III} \rangle}{dt} &= \sum_{N_\mathrm{I}, N_\mathrm{II}, N_\mathrm{III}} N_\mathrm{III} \frac{d}{dt} P(\{N_\mathrm{I}, N_\mathrm{II}, N_\mathrm{III}\}, t) \\ &= \sum_{N_\mathrm{I}, N_\mathrm{II}, N_\mathrm{III}} N_\mathrm{III} p(N_\mathrm{I}+1)(N_\mathrm{II}+1)P(\{N_\mathrm{I}+1, N_\mathrm{II}+1, N_\mathrm{III}-1\}, t) \\ &\quad - \sum_{N_\mathrm{I}, N_\mathrm{II}, N_\mathrm{III}} N_\mathrm{III} p N_\mathrm{I} N_\mathrm{II} P(\{N_\mathrm{I}, N_\mathrm{II}, N_\mathrm{III}\}, t). \quad \text{(S6)}\end{aligned}$$

Using a relationship between probabilities (N_I, N_II and N_III is taken over 0 to ∞),

$$\begin{aligned}&\sum_{N_\mathrm{I}, N_\mathrm{II}, N_\mathrm{III}} (N_\mathrm{I}+1)(N_\mathrm{II}+1) N_\mathrm{III} P(\{N_\mathrm{I}+1, N_\mathrm{II}+1, N_\mathrm{III}-1\}, t) \\ &= \sum_{N_\mathrm{I}, N_\mathrm{II}, N_\mathrm{III}} N_\mathrm{I} N_\mathrm{II} (N_\mathrm{III}+1) P(\{N_\mathrm{I}, N_\mathrm{II}, N_\mathrm{III}\}, t), \quad \text{(S7)}\end{aligned}$$

The following equation is obtained.

$$\frac{d\langle N_\mathrm{III} \rangle}{dt} = \sum_{N_\mathrm{I}, N_\mathrm{II}, N_\mathrm{III}} p N_\mathrm{I} N_\mathrm{II} P(\{N_\mathrm{I}, N_\mathrm{II}, N_\mathrm{III}\}, t) = p\langle N_\mathrm{I} N_\mathrm{II} \rangle. \quad \text{(S8)}$$

If the mean field approximation is adopted,

$$\langle N_\mathrm{I} N_\mathrm{II} \rangle \approx \langle N_\mathrm{I} \rangle \langle N_\mathrm{II} \rangle, \quad \text{(S9)}$$

the equation can be rewritten with respect to the concentration, C_X / mol $\cdot$ L^{-1}.

$$\frac{dC_\mathrm{III}}{dt} = p\upsilon N_\mathrm{Avogadro} C_\mathrm{I} C_\mathrm{II} \quad \text{where} \quad C_\mathrm{X} = \frac{\langle N_\mathrm{X} \rangle}{\upsilon N_\mathrm{Avogadro}}. \quad \text{(S10)}$$

N_Avogadro is Avogadro constant, and υ is the volume of system. Therefore, the conventional rate constant (k) is related to $p\upsilon N_\mathrm{Avogadro}$ under the mean field approximation.

3.2 Unimolecular reaction

An unimolecular reaction,

$$\text{molecule I} \rightarrow \text{molecule II}$$

is considered in a similar manner to the bimolecular reaction[1,2]. The state of the system is described by a set of molecular numbers, N_I and N_II, $\{N_\mathrm{I}, N_\mathrm{II}\}$. The master equation is written as follows using a constant r representing the rate.

$$\frac{dP(\{N_\mathrm{I}, N_\mathrm{II}\}, t)}{dt} = r(N_\mathrm{I}+1)P(\{N_\mathrm{I}+1, N_\mathrm{II}-1\}, t) - rN_\mathrm{I}P(\{N_\mathrm{I}, N_\mathrm{II}\}, t). \quad \text{(S11)}$$

The first term of the right hand side is the variation of $\{N_\mathrm{I}+1, N_\mathrm{II}-1\} \rightarrow \{N_\mathrm{I}, N_\mathrm{II}\}$, increasing the probability of $P(\{N_\mathrm{I}, N_\mathrm{II}\}, t)$. The second term is that of $\{N_\mathrm{I}, N_\mathrm{II}\} \rightarrow \{N_\mathrm{I}-1, N_\mathrm{II}+1\}$, decreasing the probability of $P(\{N_\mathrm{I}, N_\mathrm{II}\}, t)$. In both terms, population of molecule II is increased.

Similar to the bimolecular reaction, the time evolution of the mean number $\langle N_\mathrm{II} \rangle$ at time t is evaluated as,

$$\begin{aligned}\frac{d\langle N_\mathrm{II} \rangle}{dt} &= \sum_{N_\mathrm{I}, N_\mathrm{II}} N_\mathrm{II} \frac{d}{dt} P(\{N_\mathrm{I}, N_\mathrm{II}\}, t) \\ &= \sum_{N_\mathrm{I}, N_\mathrm{II}} N_\mathrm{II} r(N_\mathrm{I}+1) P(\{N_\mathrm{I}+1, N_\mathrm{II}-1\}, t) \\ &\quad - \sum_{N_\mathrm{I}, N_\mathrm{II}} N_\mathrm{II} r N_\mathrm{I} P(\{N_\mathrm{I}, N_\mathrm{II}\}, t) \\ &= \sum_{N_\mathrm{I}, N_\mathrm{II}} r N_\mathrm{II} P(\{N_\mathrm{I}, N_\mathrm{II}\}, t) = r\langle N_\mathrm{II} \rangle. \quad \text{(S12)}\end{aligned}$$

Using the concentration C_II defined in Eq. (S10), the equation is rewritten as follows.

$$\frac{dC_\mathrm{II}}{dt} = rC_\mathrm{II}. \quad \text{(S13)}$$

As a consequence, r is equivalent to the conventional rate constant.

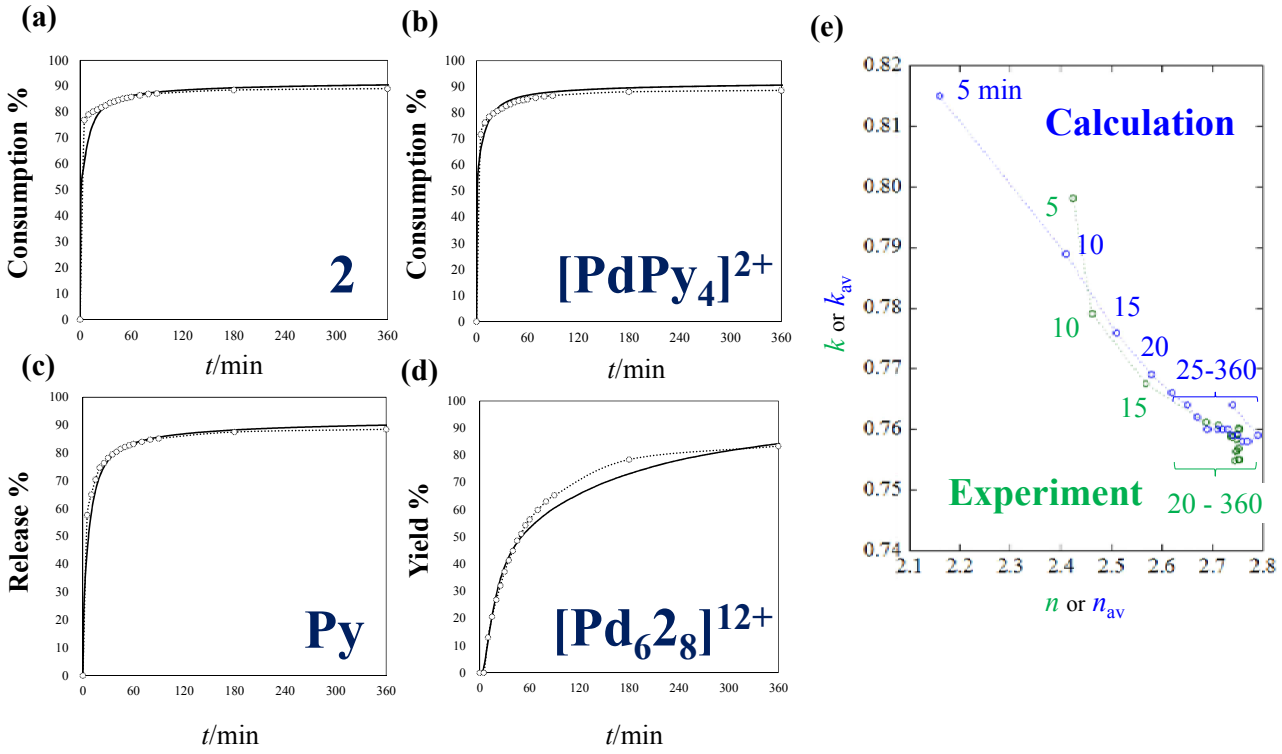

Fig. S2 Comparison between calculations (solid lines) and experimental results (circles), (a) Consumption rate of **2**, (b) Consumption rate of $[PdPy_4]^{2+}$, (c) Release rate of Py, and (d) Yield of $[Pd_6\mathbf{2}_8]^{12+}$. (e) (n,k)-analysis obtained by calculations (blue circles) and experimental results (green circles).

4 Computational details

4.1 Reactions

In the present study, all the reactions on the self-assembly process are classified into the following four types of ligand exchange reactions. Pd-L bond formation accompanies Py relase.

(i) Intermolecular Pd-L bond formation between $[Pd_aL_bPy_c]^{2a+}$ ($b \neq 0$) and L.

$$[Pd_aL_bPy_c]^{2a+} + L \rightarrow [Pd_aL_{b+1}Py_{c-1}]^{2a+} + Py$$

(ii) Intermolecular Pd-L bond formation except for (i). $a \neq 0$ and $a' \neq 0$ or $b = 0$.

$$[Pd_aL_bPy_c]^{2a+} + [Pd_{a'}L_{b'}Py_{c'}]^{2a'+} \rightarrow [Pd_{a+a'}L_{b+b'}Py_{c+c'-1}]^{2(a+a')+} + Py$$

(iii) Back reaction of (i) and (ii).

$$[Pd_{a+a'}L_{b+b'}Py_{c+c'-1}]^{2(a+a')+} + Py \rightarrow [Pd_aL_bPy_c]^{2a+} + [Pd_{a'}L_{b'}Py_{c'}]^{2a'+}$$

(iv) Intramolecular Pd-L bond formation.

$$[Pd_aL_bPy_c]^{2a+} \rightarrow [Pd_aL_bPy_{c-1}]^{2a+} + Py$$

(iv′) Intramolecular Pd-L bond formation in the final step.

$$[Pd_6L_8Py]^{12+} \rightarrow [Pd_6L_8]^{12+} + Py$$

While the first three are bimolecular reactions whose rate in the master equation is expressed as pN_AN_B, (iv) and (iv′) unimolecular reaction with the rate of rN_A.

4.2 Parameters

Unfortunately, an accurate estimation of transition rate in this system is infeasible, and there is no way to uniquely determine the parameters. Nevertheless, the time scale of ligand exchange reaction can be rationalized as follows. Now, we have rate constant value of the ligand exchange reaction between Py in $[PdPy_4]^{2+}$ and free Py, $k_{\mathrm{ref}} = 1.9 \pm 0.14 \times 10^{-2}\ \mathrm{s}^{-1}$, evaluated in experiments, which is related to reaction (i) of the present system. Assuming bimolecular process (Eq. (S10)) for this reaction, the parameter of rate in master equation, p, is related to k_{ref} by $(p\upsilon N_{\mathrm{A}})\cdot C_{\mathrm{X}} \approx k_{\mathrm{ref}}$. Since $C_{\mathrm{X}}\upsilon N_{\mathrm{A}} \approx N_{\mathrm{X}} \approx 10^2$ in the present computation, rough estimate is obtained $p \approx k_{\mathrm{ref}}/(C_{\mathrm{X}}\upsilon N_{\mathrm{A}}) \approx 10^{-4}\ \mathrm{s}^{-1} \approx 10^{-2}\ \mathrm{min}^{-1}$. Parameters for intermolecular reactions (ii) and (iii) are reasonably set to be the same order of (i). Intramolecular process (iv) is assumed to be faster while the rate-determining step (iv′) must be slower. As a consequence, the used parameters for each type are summarized as follows; (i) $p_{\mathrm{L}} = 2.25 \cdot 10^{-2}\ \mathrm{min}^{-1}$, (ii) $p = 1.5 \cdot 10^{-2}\ \mathrm{min}^{-1}$, (iii) $q = 1.2 \cdot 10^{-2}\ \mathrm{min}^{-1}$, and (iv) $p_{\mathrm{E}} = 6.0\ \mathrm{min}^{-1}$. For (iv′), 70% of the reaction was assigned to $p_{\mathrm{f}} = p_{\mathrm{E}}$ and 30% was to $p'_{\mathrm{f}} = 2.4 \cdot 10^{-3}\ \mathrm{min}^{-1}$. Note that the parameter for the bimolecular reactions (i)–(iii) is different from the conventional

rate constant as described in section 3.

As the initial condition, the total numbers of Pd, L and Py were respectively 300, 400 and 1200. Only reactants $[PdPy_4]^{2+}$ and L were prepared in the system. We confirmed that these numbers were enough to obtain converged results. 10^3 trajectories were then collected to achieve enough statistical accuracy.

5 Self-assembly system using another tridentate ligand

In the experiment[6], reactions with two different tridentate ligands (L = **1** or **2**) were examined. The **2** was introduced by changing three Me groups of **1** (in main manuscript) to deuterium. The deuterium system is described using parameters: (i) $p_L = 4.5 \cdot 10^{-3}$ min^{-1}, (ii) $p = 3.0 \cdot 10^{-3}$ min^{-1}, (iii) $q = 6.0 \cdot 10^{-3}$ min^{-1}, and (iv) $p_E = 30$ min^{-1}. For (iv$'$), $p_f = p_E$ (60%) and $p_f' = 6.0 \cdot 10^{-3}$ min^{-1} (40%). The reaction was analyzed in the same way to **1** case, and the results are shown in Figures (S2)-(S4).

5.1 Comparison between 1 and 2: Intermolecular reaction

Only small modification was found to be adequate for the parameter in reaction type (ii), p, which determine the overall time scale in the reaction. The values are $1.5 \cdot 10^{-2}$ and $3.0 \cdot 10^{-3}$ min^{-1} for the ligand **1** and **2** systems. If the difference of these values is converted to difference of energy barrier, that is only 1 kcal/mol at ambient temperature. One plausible origin of the difference is the attractive interactions between species which enhance the frequency of intermolecuar collisions. The intermolecular interactions can be changed by the types of tridentate ligand, and in fact, the L-L attractive interactions can be enhanced by Me groups in **1**[7], which leads to faster rate of **1** system.

The parameters in reaction type (i) and (iii), q and p_L, have similar values to p. The ratio q/p determines the balance between break and formation of Pd-L bond. If $q/p < 1$, Pd-L bond formation is faster than break. This ratio critically effects on the consumption rate of metal and tridentate ligand at long time, and this long time behavior was used as a criteria for the parameter determination. The values of q/p are 0.8 and 2.0 for **1** and **2** systems. The smaller value for **1** system can be interpreted as a result of the suppression on Pd-L bond break due to the L-L stabilization effects by Me groups.

The ratio p_L/p is related to an enhancement on rates for the reaction of tridentate monomer and $[Pd_aL_bPy_c]^{2a+}$ ($b \neq 0$). This modification was found to be necessary to reproduce the rapid convergent of k_{av} value to long time limit in comparable extent to the convergence of n_{av}. The values of p_L/p are 1.5 for both systems, which effectively represents the enhanced L attachment to $[Pd_aL_bPy_c]^{2a+}$ ($b \neq 0$). One plausible origin is the attractive interaction between L monomer and multi L blocks in the latter species. L monomer can get most large attraction because the steric effects, which restrict the orientation to interact, become large in case of two large complexes.

5.2 Comparison between 1 and 2: Intramolecular reaction

For the present dilute solution, the frequency of intramolecular processes is expected to be much faster than intermolecular processes. However, the structural restrictions due to the cluster formation have a possibility to generate energy cost slowing down the process. The values of p_E in reaction type (iv), which determine the overall time evolution in addition to p, are 6.0 and 30 min^{-1} for **1** and **2** systems. The corresponding ratios, p_E/p, are 400 and 10000. The p_E of **1** system is smaller than **2** which can be interpreted that the stabilization of L-L interactions by Me groups in the cluster is weakened at disordered transition state causing the relative high energy barrier, in a consistent way to parameters in the intermolecular reaction.

Another competitive path at final step were found to be essential to reproduce not only the slowing down of reaction at final step observed in experiment[6] but also the multi-exponential time evolution of product formation, which corresponds to the reaction type (iv$'$). The values of p_f'/p_E are $4.0 \cdot 10^{-4}$ and $2.0 \cdot 10^{-4}$ min^{-1} for **1** and **2** systems, which show very slow routes although the converted energy differences are only 5 kcal/mol at ambient temperature for both ratios. This elaborated treatment is necessary since all pathways have to go through this as a final step and the rigidity of this almost completed cluster limit the reversibility which prevent fast escape from the kinetic trapping. The detailed feature is enhanced to some extent because the experiment is performed in lower temperature than usual high temperature in self-assembly[6]. Hence, the simple reaction model may become more reliable at high temperature where the experimental observation is very difficult. The percentages of the path branch are expected to reflects the complicated histories of geometrical isomers before leading to the $[Pd_6L_8Py]^{12+}$, and were simply determined to reproduce the time evolution of product formation.

Preliminary model calculations based on quantum chemistry were performed to address the structure of $[Pd_6\mathbf{1}_8Py]^{12+}$ isomers. We found at least two very different structures related to the present issue.

References

1 M. R. D'Orsogna, G. Lakatos, and T. Chou, J. Chem. Phys. **136**, 084110, (2012).

2 M. R. D'Orsogna, B. Zhao, B. Berenji, and T. Chou, J. Chem. Phys. **139**, 121918, (2013).

3 P. L. Krapivsky, E. Ben-Naim, and S. Redner, *Statistical Physics of Irreversible Processes,* Cambridge University Press, Cambridge, England, 2010.

4 A. B. Bortz, M. H. Kalos, and J. L. Lebowitz, J. Comput. Phys. **17**, 10, (1975).

5 D. T. Gillespie, Annu. Rev. Phys. Chem. **58**, 35, (2007).

6 Y. Tsujimoto, T. Kojima, and S. Hiraoka, Chem. Sci. **5**, 4167, (2014).

7 J. Koseki, Y. Kita, S. Hiraoka, U. Nagashima, and M. Tachikawa, Theor. Chem. Acc. **130**, 1055, (2011).

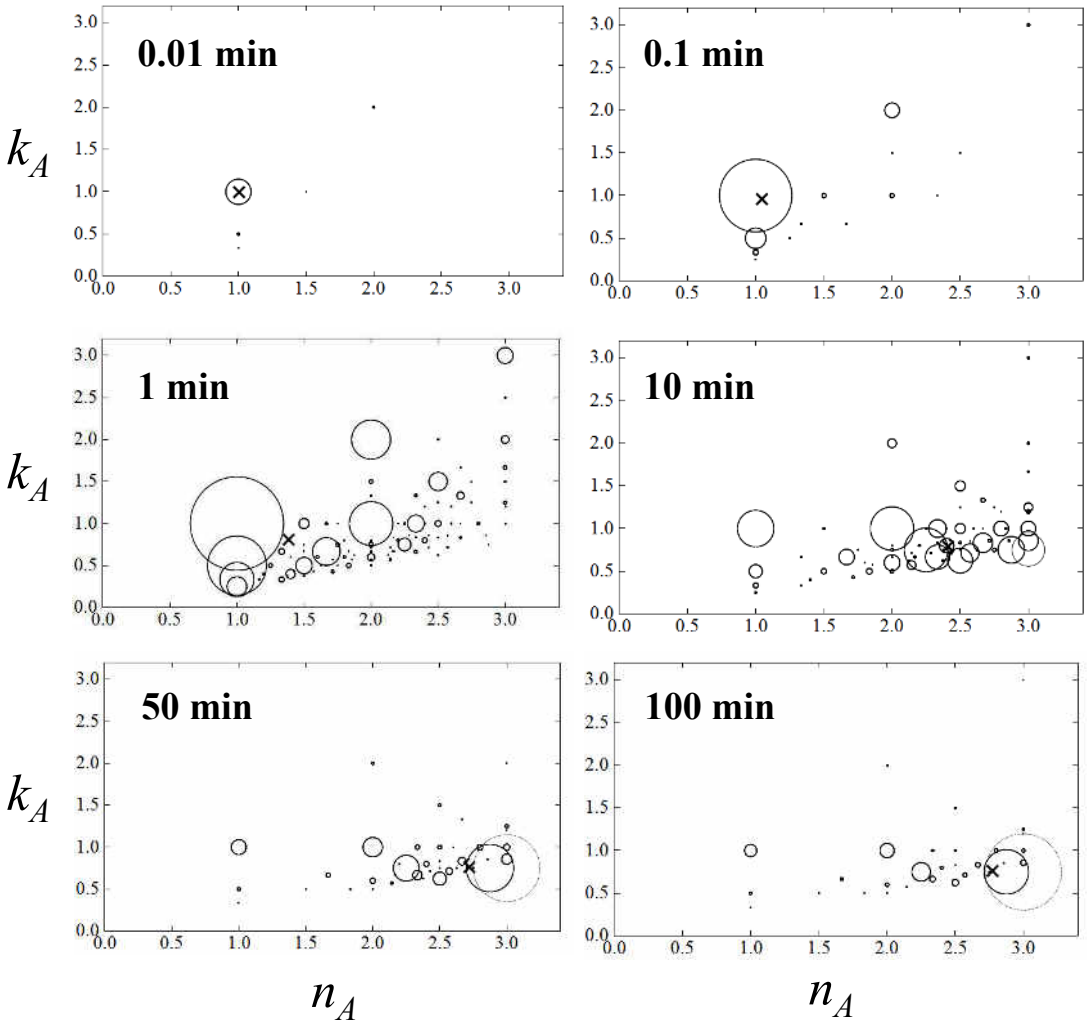

Fig. S3 Calculated distributions of (n_A, k_A) for intermediate species. $(n_{\mathrm{av}}, k_{\mathrm{av}})$ values are shown by X mark. The dotted circle denotes the distribution of the product. The radius of circle equals $0.05\sqrt{\langle N_A(t)\rangle}$.

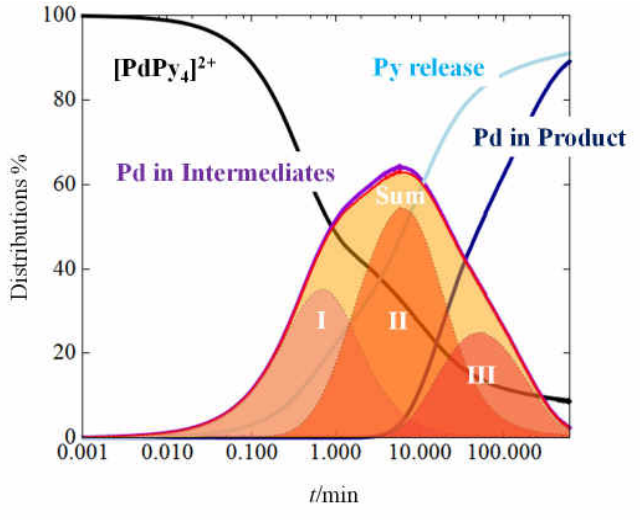

Fig. S4 Distributions of Pd in reactant, Group I-III, their sum, all of the intermediates, product. The distribution of released Py is also shown.